Study of Ring-open Fragmentation in Two Rosane-type Diterpenoid Lactones by ESI-MS^n (quadrupole time-of-flight and ion trap)

Tian-shan WANG

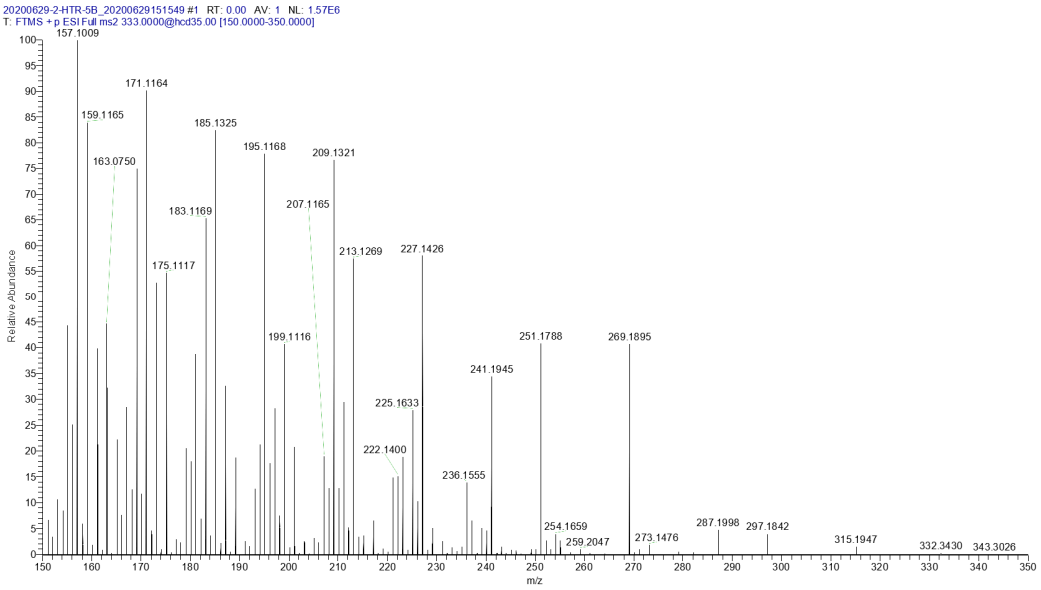

Figure S1. High resolution MS/MS spectrum of *m/z* 333 of 11β-hydroxyrosenonolactone (**1**)

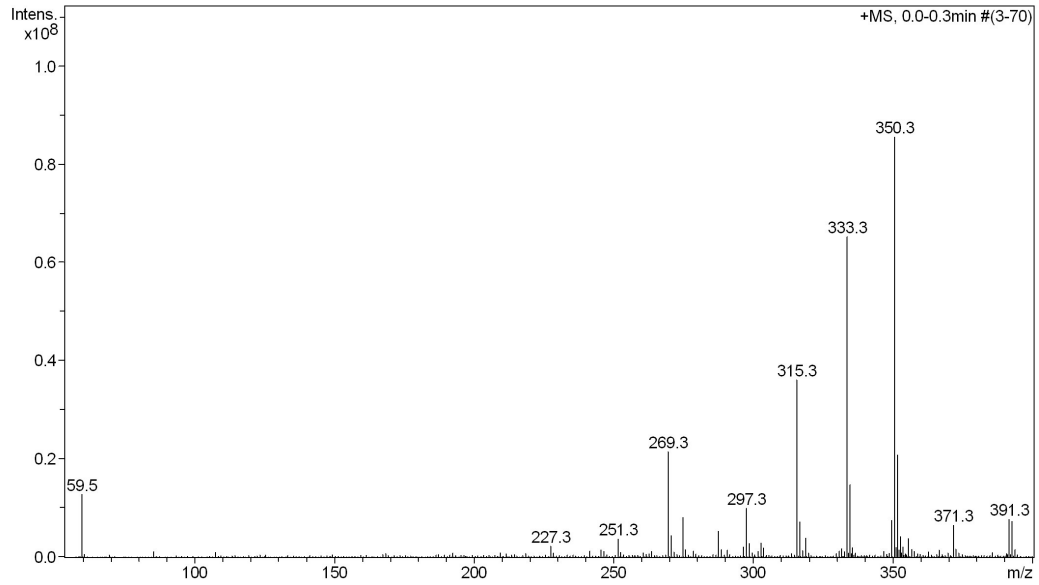

Figure S2. ESI-MS spectrum of 11β-hydroxyrosenonolactone (**1**)

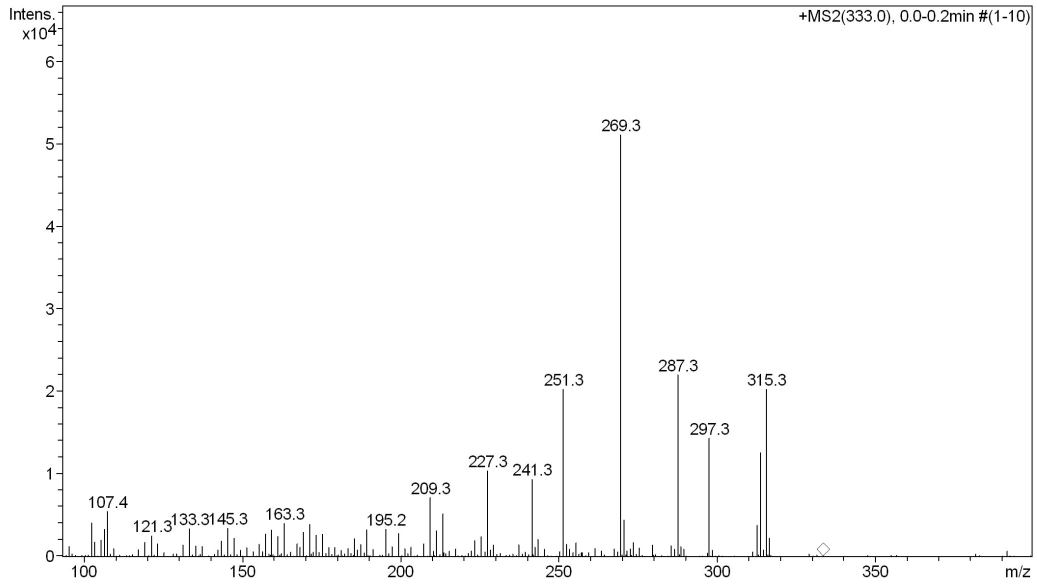

Figure S3. MS^2 spectrum of *m/z* 333 of 11β-hydroxyrosenonolactone (**1**)

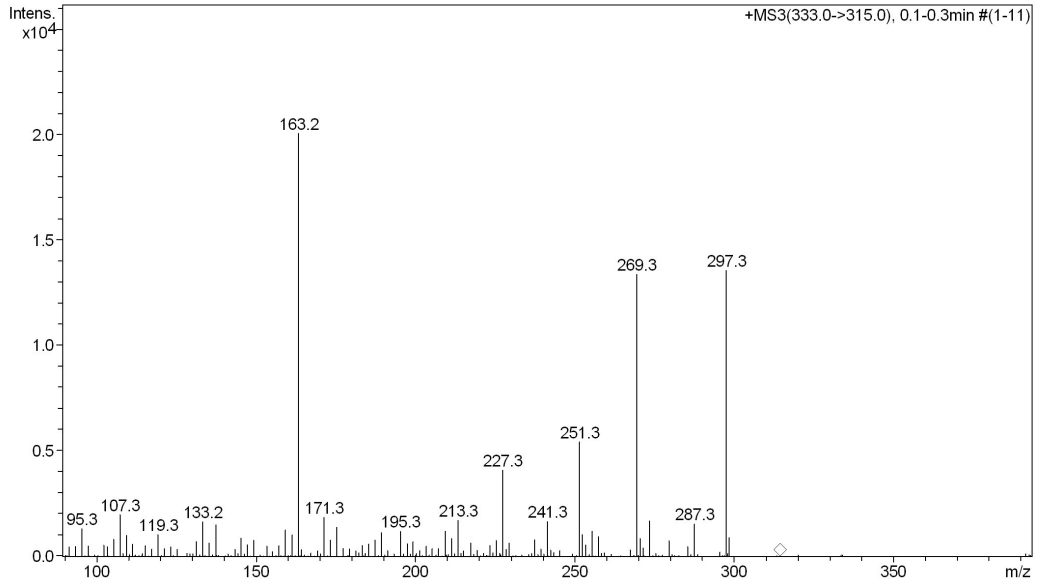

Figure S4. MS^3 spectrum of *m/z* 333→315 of 11β-hydroxyrosenonolactone (**1**)

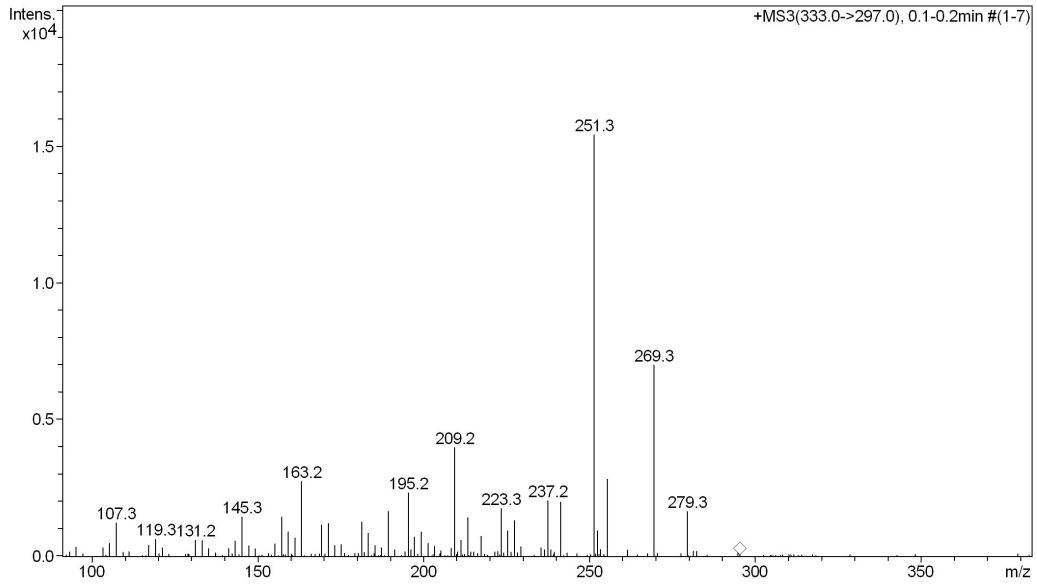

Figure S5. MS^3 spectrum of *m/z* 333→297 of 11β-hydroxyrosenonolactone (**1**)

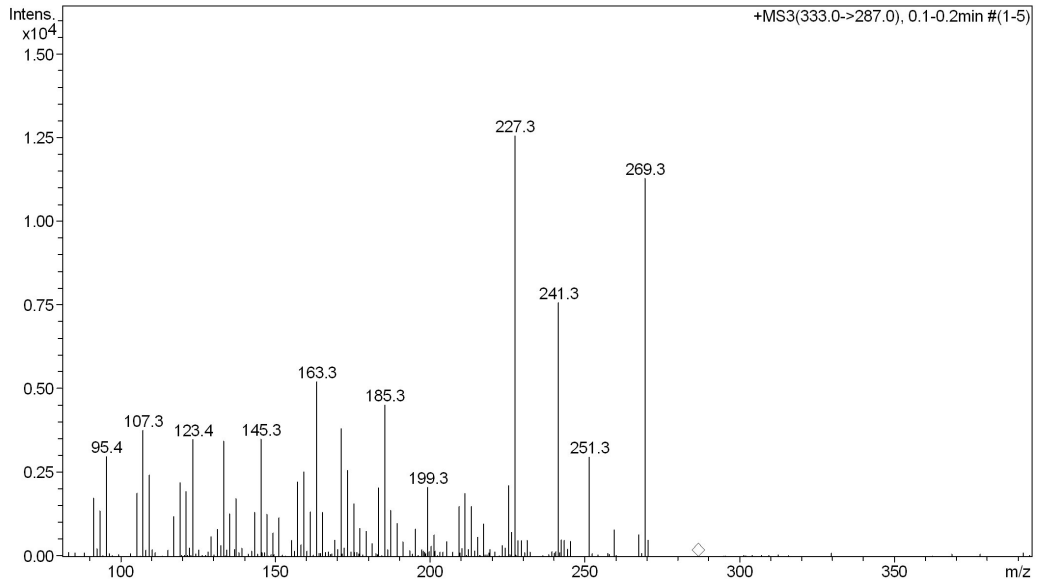

Figure S6. MS^3 spectrum of *m/z* 333→287 of 11β-hydroxyrosenonolactone (**1**)

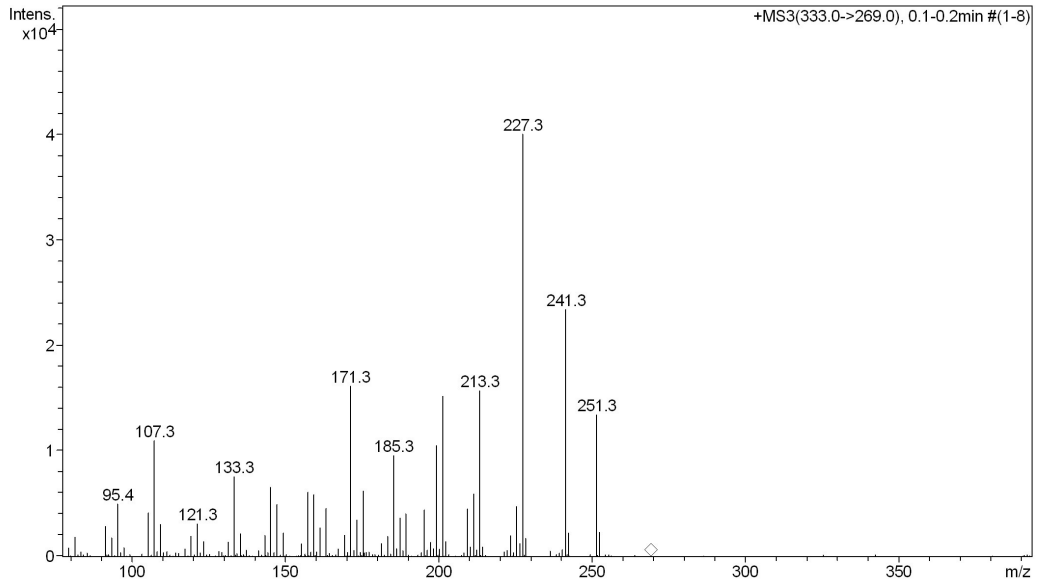

Figure S7. MS^3 spectrum of *m/z* 333→269 of 11β-hydroxyrosenonolactone (**1**)

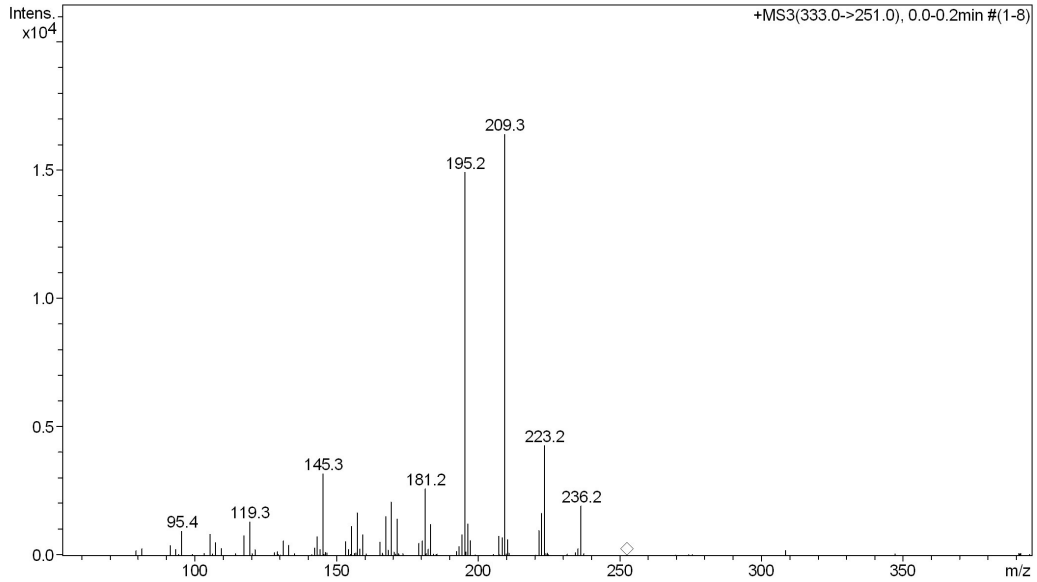

Figure S8. MS^3 spectrum of *m/z* 333→251 of 11β-hydroxyrosenonolactone (**1**)

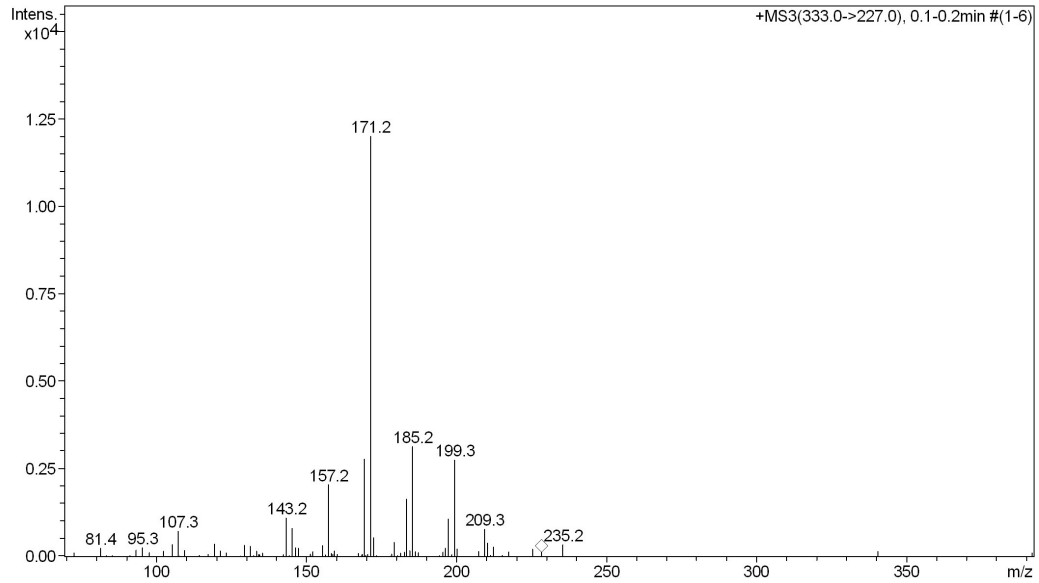

Figure S9. MS^3 spectrum of *m/z* 333→227 of 11β-hydroxyrosenonolactone (**1**)

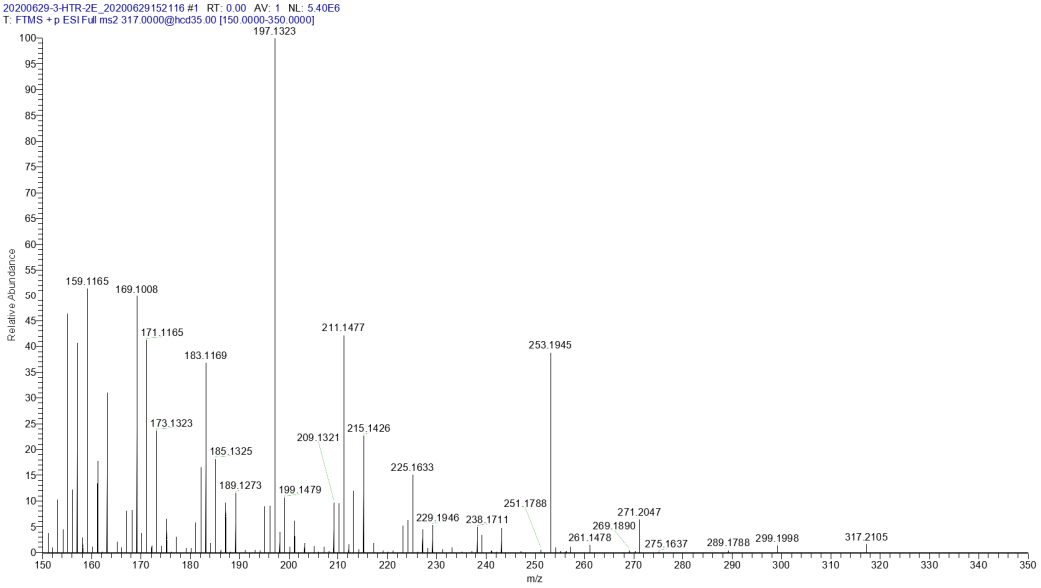

Figure S10. High resolution MS/MS spectrum of *m/z* 317 of rosenonolactone (**2**)

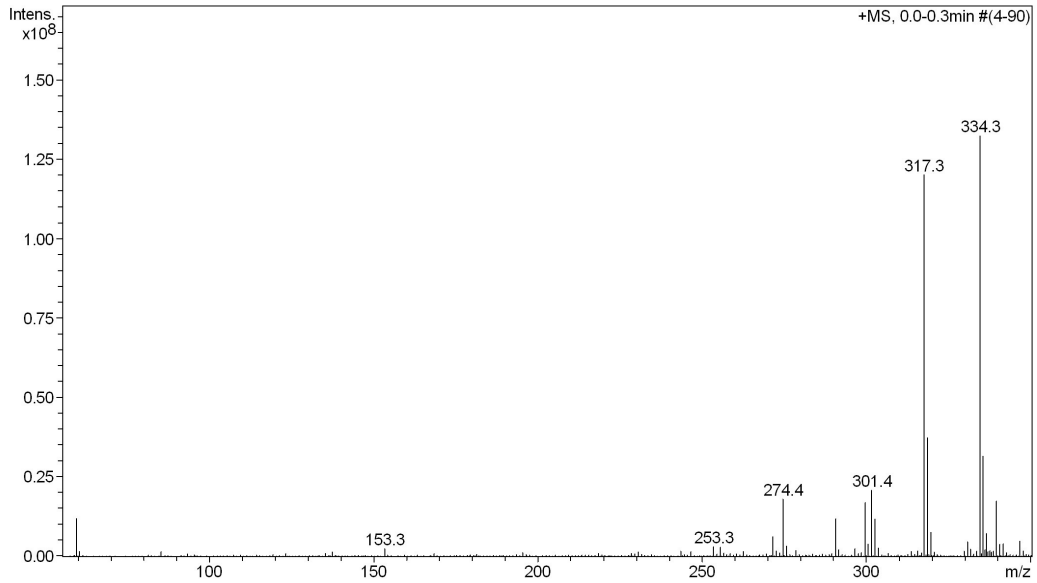

Figure S11. ESI-MS spectrum of rosenonolactone (**2**)

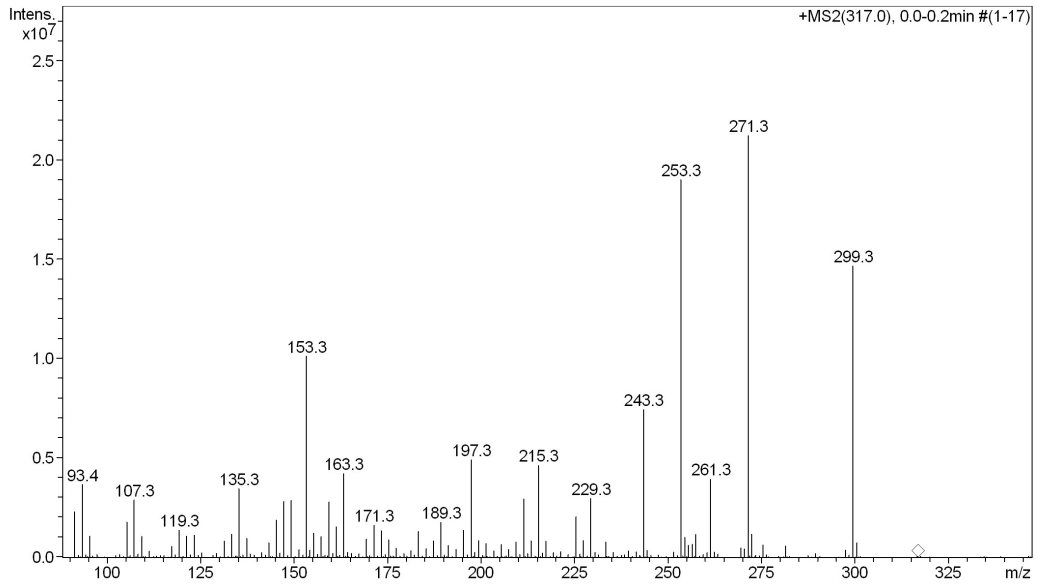

Figure S12. MS^2 spectrum of *m/z* 317 of rosenonolactone (**2**)

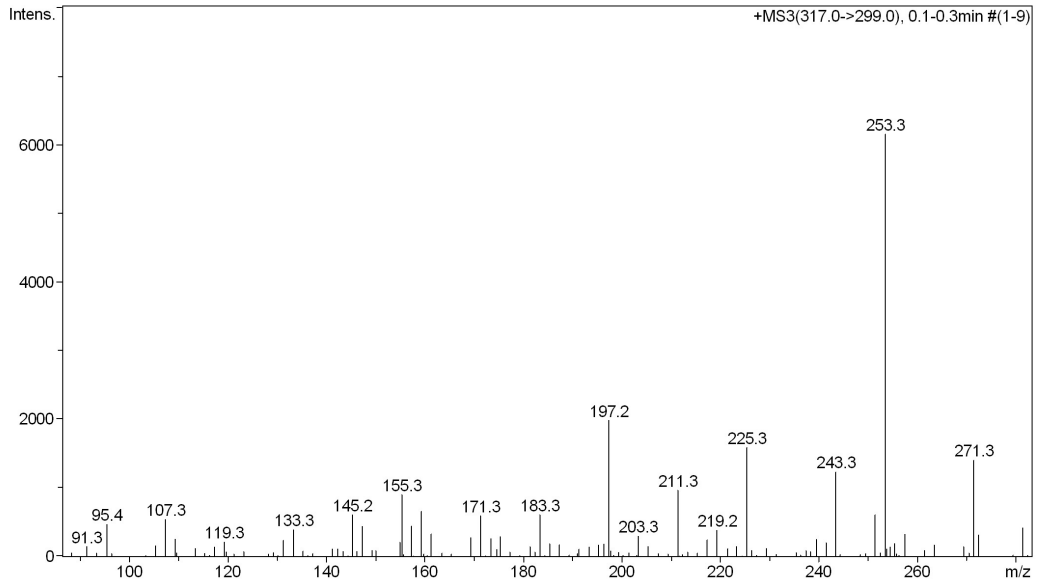

Figure S13. MS^3 spectrum of *m/z* 317→299 of rosenonolactone (**2**)

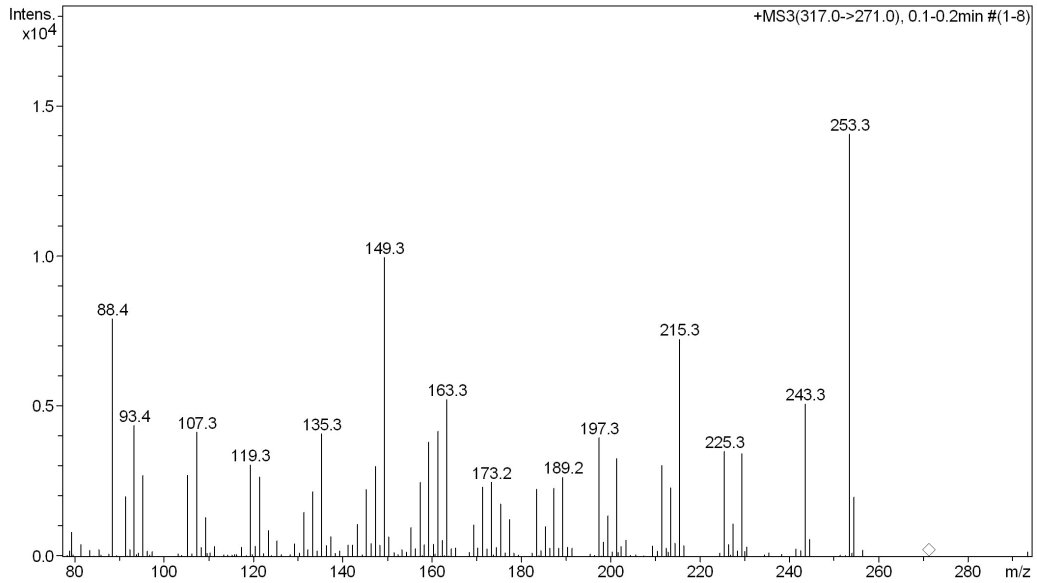

Figure S14. MS^3 spectrum of *m/z* 317→271 of rosenonolactone (**2**)

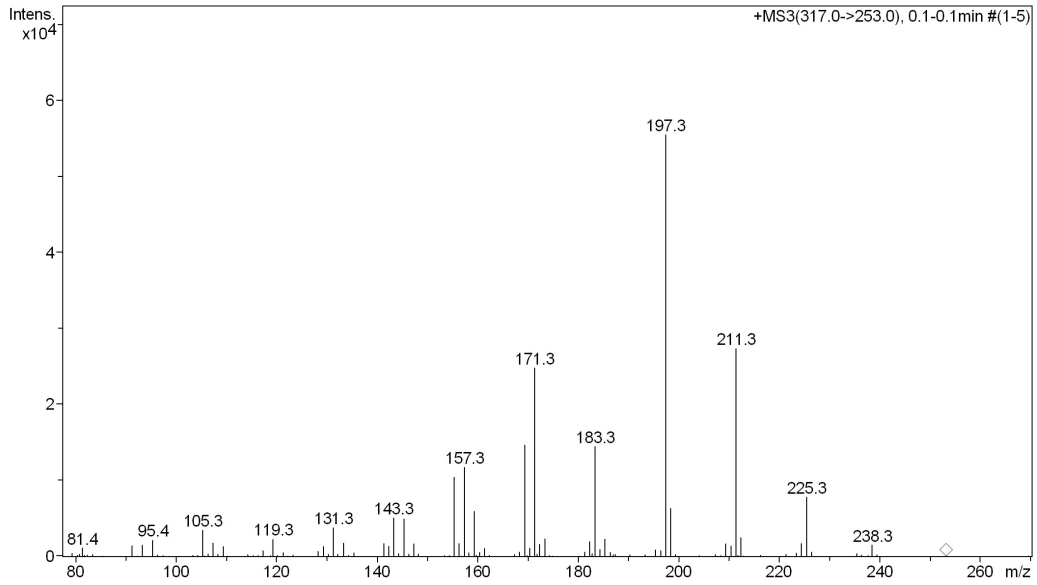

Figure S15. MS^3 spectrum of *m/z* 317→253 of rosenonolactone (**2**)

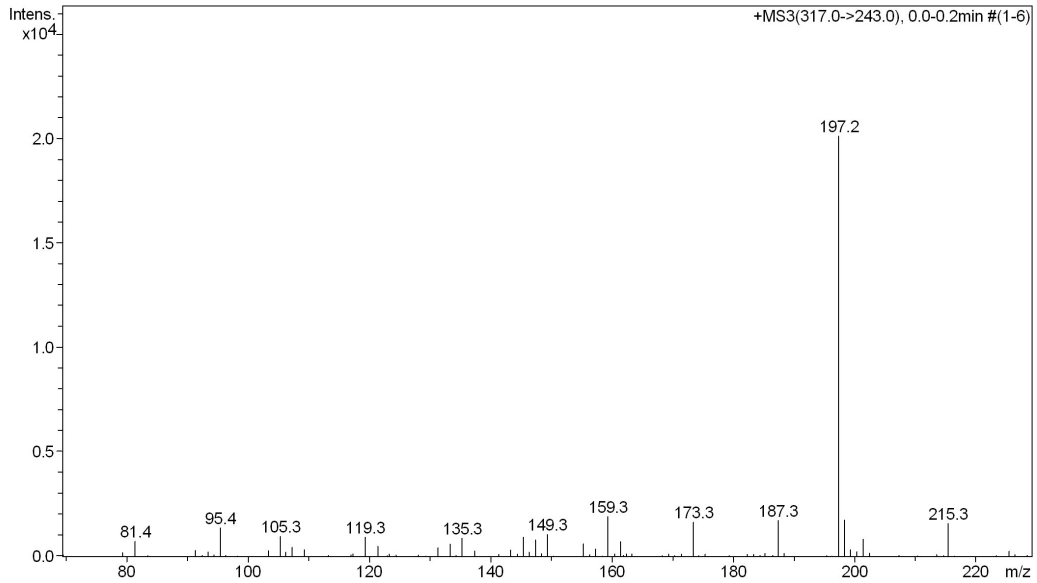

Figure S16. MS^3 spectrum of *m/z* 317→243 of rosenonolactone (**2**)

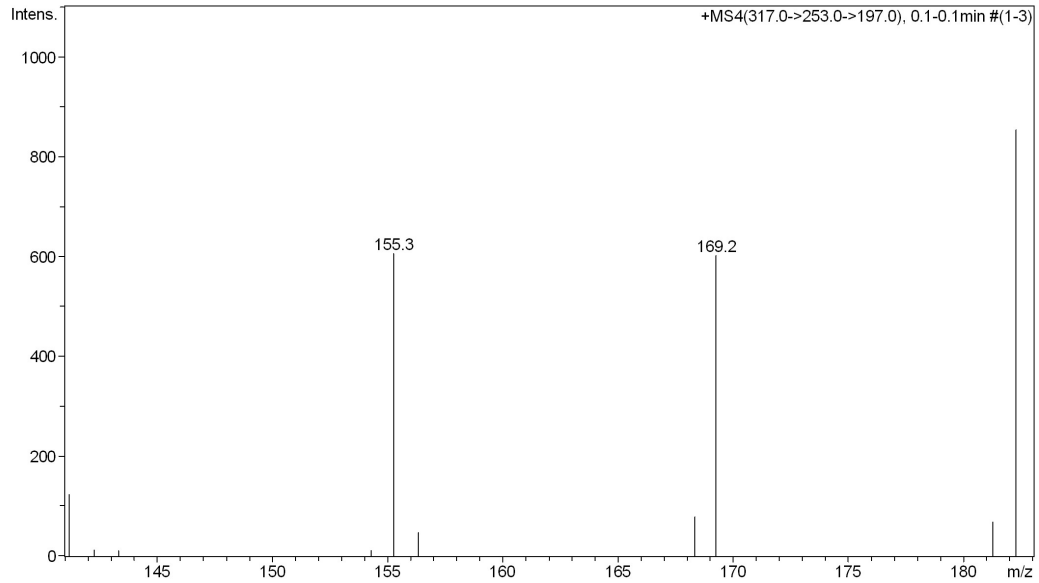

Figure S17. MS^4 spectrum of *m/z* 317→253→197 of rosenonolactone (**2**)